Robust Timing Epoch Tracking for Alamouti Space-Time Coding in Flat Rayleigh Fading MIMO Channels

Pawel A. Dmochowski, Peter J. McLane
Department of Electrical and Computer Engineering
Queen's University, Kingston, ON, K7L 3N6, Canada
Email: {dmochowp,mclane}@ee.queensu.ca

***Abstract*— We propose a very low complexity timing error detector for $n_T = 2$ orthogonal space-time block coded M-PSK systems with an arbitrary number of receive antennas. The algorithm uses maximum-likelihood detection variables to estimate the timing error by examining the difference in threshold crossings, similarly to the Mueller and Muller Detector. We show that the timing error estimation is independent of the channel state, thus making it very robust in poor channel conditions. The decision directed version of the detector is used to evaluate the tracking performance for BPSK and QPSK signaling in 1-, 2- and 4-receive antenna systems. Symbol error rate as well as mean square estimation error results are presented. We examine the performance as a function of the timing drift and show that the receiver is able to maintain lock up to a normalized timing bandwidth of $B_\tau T = 0.001$. Complete channel state estimation is assumed throughout the paper.**

I. Introduction

The emergence of multiple input multiple output (MIMO) systems has allowed for an increase in the data rate and the capacity of wireless links. In particular, the theory of orthogonal space time block coding (OSTBC) has received a lot of attention since its development [1]–[3], due to its ability to provide maximum diversity in fading environments while maintaining low decoding complexity.

As in conventional, single-antenna synchronous communication, the receiver's ability to synchronize the timing epoch is critical to the overall performance of MIMO systems. The problem of timing acquisition in space-time coded modems was first addressed in [4], where the receiver obtained timing information by maximizing the oversampled approximated log-likelihood function (LLF), which in turn was derived from orthogonal training sequences. It has been shown [5] [6], that the algorithm in [4] is highly sensitive to the oversampling ratio Q, specifically that the mean square error (MSE) of the estimation is lower bounded by $1/(12Q^2)$. A modification of the method in [4] was presented in [5] and [6] where the resulting algorithm significantly reduces the oversampling required to achieve a given MSE.

The work outlined above deals with the problem of initial timing acquisition using a preamble of known training symbols. In this paper we focus on the task of tracking the timing in multiple antenna systems once initial acquisition has been performed. Previous work in [7] dealt with timing tracking for receive antenna diversity only. Here, we present a method suited for 2-transmit antenna OSTBC M-PSK systems. Specifically we derive a very low-complexity timing error detector (TED), similar in structure to that proposed in [8], but operating on OSTBC maximum likelihood (ML) detection variables. We show that the proposed TED possesses an attractive property of being independent of the channel state, and as a result, its performance is very robust to the effects of fading. This result, and all the results in the paper, assume complete channel state information being available at the receiver. Performance results are presented for the decision-directed (DD) version of the TED. We evaluate the symbol error rate (SER) as well as timing MSE for BPSK and QPSK signaling for systems with 1, 2 and 4 receive antennas.

The remainder of the paper is organized as follows. System overview and assumptions are described in Section II. The proposed timing error detector is derived in Section III, while timing error correction is discussed in Section IV. Sections V-A and V-B present the SER performance, and the effects of increased timing bandwidth. Section V-C presents MSE results. Finally, we conclude the paper with a summary of the findings in Section VI.

II. System Overview

We consider a communication system comprising of n_T transmit and n_R receive antennas employing orthogonal space-time block coding. The transmitter encodes N_s M-PSK information symbols and transmits them over n_T antennas in N time slots, resulting in a code rate of $R = N_s/N$. We denote the lth $n_T \times N$ code block by $\mathbf{X}_l$ and its ik entry by $x_i(lN+k)$. Note that l is the code block index, $k = 0, \ldots, N-1$ is the time slot index within the block and $i = 1, \ldots, n_T$ is the transmit antenna index. Let the information symbols used to encode block $\mathbf{X}_l$ be given by a_m^l, where $m = 0, \ldots, N_s - 1$ is their index within the block. Then, $\mathbf{X}_l$ is given by the linear combination of a_m^l and their conjugates [9]

$$\mathbf{X}_l = \sum_{m=0}^{N_s-1} \Re\{a_m^l\}\mathbf{A}_m + i\Im\{a_m^l\}\mathbf{B}_m, \tag{1}$$

where the operators $\Re\{\cdot\}$ and $\Im\{\cdot\}$ return the real and imaginary parts of their arguments, and $\mathbf{A}_m$ and $\mathbf{B}_m$ are code matrices of dimension $n_T \times N$. For $n_T = 2$, that is the scheme proposed by Alamouti [1], $\mathbf{A}_m$ and $\mathbf{B}_m$ are given by [9]

$$\mathbf{A}_0 = \begin{bmatrix} 1 & 0 \\ 0 & 1 \end{bmatrix}, \mathbf{A}_1 = \begin{bmatrix} 0 & -1 \\ 1 & 0 \end{bmatrix} \tag{2}$$

and

$$\mathbf{B}_0 = \begin{bmatrix} 1 & 0 \\ 0 & -1 \end{bmatrix}, \mathbf{B}_1 = \begin{bmatrix} 0 & 1 \\ 1 & 0 \end{bmatrix}. \tag{3}$$

Following the encoding, data on each transmit antenna is passed through a pulse shaping filter. The pulse shaping is split between the transmitter and receiver, each employing a root raised cosine (RRC) filter with a rolloff factor of β. The combined Nyquist raised cosine pulse is denoted by $g(t)$.

We assume a quasi-static frequency-flat Rayleigh fading channel modeled by a matrix $\mathbf{H}$ of dimension $n_R \times n_T$, with entries h_{ij} corresponding to the state of the channel from ith transmit to jth receive antenna. We also denote the jth row of $\mathbf{H}$ by a vector $\mathbf{h}_j = [h_{1j}, h_{2j}, \ldots, h_{n_T j}]$. The channel state h_{ij} is a complex Gaussian random variable, assumed to be independent and identically distributed (iid) for all i and j. U-shaped power spectrum characteristic of isotropic scattering is assumed, and thus the autocorrelation function of h_{ij} (for all i and j) is given by [10]

$$R_h(\xi) = \sigma_h^2 J_0(2\pi f_D \xi), \tag{4}$$

where σ_h^2 is the variance of the random process, and $J_0(x)$ denotes the Bessel function of the first kind of order zero. The quantity f_D in (4) denotes the maximum Doppler frequency.

Assuming quasi-static fading, the received signal at antenna j is given by

$$r_j(t) = \sum_{i=1}^{n_T} h_{ij} \sum_n x_i(n) g(t - nT + \epsilon(t)) + \eta_j(t), \tag{5}$$

where $\eta_j(t)$ is a zero mean complex Gaussian noise and $\epsilon(t)$ is the unknown timing offset assumed to be equal at all receiver branches. Note that the channel is assumed to be constant for the duration of the intersymbold interference (ISI) contributing terms in the inner summation of (5). Consider the sampled signal corresponding to time slots $k = 0, \ldots, N-1$ within a single block l, and let $r_j^l(k) \triangleq r_j((lN+k)T)$ and $\eta_j^l(k) \triangleq \eta_j((lN+k)T)$. Without the loss of generality we consider the block $l = 0$, and for notational convenience we drop the block index superscript for the remainder of the derivation. Assuming that the timing offset is constant for the duration of one block, using (5) we can express the received symbols by

$$r_j(k) = \sum_{i=1}^{n_T} h_{ij} \tilde{x}_i(k, \epsilon) + \eta_j(k), \tag{6}$$

where $\tilde{x}_i(k, \epsilon)$ is given by

$$\tilde{x}_i(k, \epsilon) = \sum_n x_i(n) g(kT - nT + \epsilon).$$

The quantity $\tilde{x}_i(k, \epsilon)$ is the equivalent kth transmitted symbol from antenna i given the ISI caused by the sampling error ϵ. We can express (6) in matrix notation by

$$r_j(k) = \mathbf{h}_j \tilde{\mathbf{x}}_\epsilon(k) + \eta_j(k), \tag{7}$$

where $\tilde{\mathbf{x}}_\epsilon(k) = [\tilde{x}_1(k,\epsilon), \ldots, \tilde{x}_{n_T}(k,\epsilon)]^T$ and $\mathbf{h}_j$ is the jth row of $\mathbf{H}$. To aid further derivation, it is convenient to express $\tilde{\mathbf{x}}_\epsilon(k)$ in terms of data blocks transmitted, that is

$$\tilde{\mathbf{x}}_\epsilon(k) = \sum_{l'} \mathbf{X}_{l'} \mathbf{g}_\epsilon(k - l'N), \tag{8}$$

where the summation is taken over the blocks contributing to ISI and $\mathbf{g}_\epsilon(k)$ is a column vector of pulse samples

$$\mathbf{g}_\epsilon(k) = [g(kT + \epsilon), \ldots, g((k - N + 1)T + \epsilon)]^T.$$

Finally, a row vector of all N received symbols for one code block at antenna j is given by

$$\mathbf{r}_j = \mathbf{h}_j \tilde{\mathbf{X}}_\epsilon + \boldsymbol{\eta}_j,$$

where $\mathbf{r}_j = [r_j(0), \ldots, r_j(N-1)]$, the $n_T \times N$ matrix $\tilde{\mathbf{X}}_\epsilon = [\tilde{\mathbf{x}}_\epsilon(0), \ldots, \tilde{\mathbf{x}}_\epsilon(N-1)]$ and $\boldsymbol{\eta}_j$ is a noise row vector. The receiver forms ML detection variables for each information symbol within a block, which can be expressed, for $m = 0, \ldots, N_s - 1$, by [9]

$$\tilde{s}_m = \frac{1}{\|\mathbf{H}\|^2} \left[\Re\{tr(\mathbf{Y}^H \mathbf{H} \mathbf{A}_m)\} - i\Im\{tr(\mathbf{Y}^H \mathbf{H} \mathbf{B}_m)\} \right], \tag{9}$$

where tr denotes the trace operator, $\|\mathbf{H}\|$ is the Frobenius norm of $\mathbf{H}$ and $\mathbf{Y}$ is an $n_R \times N$ matrix whose jth row is $\mathbf{r}_j$. The projection of $\tilde{s}_m$ onto the signal constellation then forms the detected information symbols denoted by $\hat{a}_m$

III. Timing Error Detector

We now present a method for estimating the timing error in $n_T = 2$ OSTBC systems with an arbitrary number of receive antennas. The proposed TED uses the ML detection variables given by (9) to estimate the timing error using the difference in threshold crossings. We show that it possesses a key feature of being insensitive to channel fading.

Consider an estimate of the timing error in the form of

$$\hat{\epsilon} = a_0 \tilde{s}_1 - a_1 \tilde{s}_0, \tag{10}$$

where once again we consider block $l = 0$ and drop the block index for the sake of simplicity. We examine the properties of (10) by considering $E\{\hat{\epsilon}\}$, where the expectation is taken over the information symbols a_m and the noise.

Referring to (9), let $\boldsymbol{\Lambda} = \mathbf{Y}^H \mathbf{H}$, and denote its entries by $\lambda_{ik'}$, where $i = 1, \ldots, n_T$ and $k' = k + 1 = 1, \ldots, N$ is the shifted time index within a block. It is easily shown that

$$\lambda_{ik'} = \sum_{j=1}^{n_R} r_j^*(k'-1) h_{ij}. \tag{11}$$

For $n_T = 2$, the quantities $tr(\boldsymbol{\Lambda}\mathbf{A}_m)$ and $tr(\boldsymbol{\Lambda}\mathbf{B}_m)$, $m = 0, 1$, are given by

$$\begin{aligned} tr(\boldsymbol{\Lambda}\mathbf{A}_0) &= \lambda_{11} + \lambda_{22} \\ tr(\boldsymbol{\Lambda}\mathbf{A}_1) &= \lambda_{21} - \lambda_{12} \\ tr(\boldsymbol{\Lambda}\mathbf{B}_0) &= \lambda_{11} - \lambda_{22} \\ tr(\boldsymbol{\Lambda}\mathbf{B}_1) &= \lambda_{21} + \lambda_{12} \end{aligned}$$

and thus

$$\tilde{s}_0 = \frac{1}{\|\mathbf{H}\|^2}(\lambda_{11}^* + \lambda_{22})$$

and

$$\tilde{s}_1 = \frac{1}{\|\mathbf{H}\|^2}(\lambda_{21}^* - \lambda_{12}).$$

Note that from (7) and (11)

$$\lambda_{ik'} = \sum_{j=1}^{n_R} h_{ij}\mathbf{h}_j^* \tilde{\mathbf{x}}_\epsilon^*(k) + \nu_{ij}(k), \tag{12}$$

where $\nu_{ij}(k) = h_{ij}\eta_j^*(k)$ is a zero mean complex Gaussian random variable. For notational convenience we let

$$\boldsymbol{\hbar}_i = \sum_{j=1}^{n_R} h_{ij}\mathbf{h}_j^*. \tag{13}$$

Then

$$E\left\{a_m \lambda_{ik'}\right\} = E\left\{a_m \boldsymbol{\hbar}_i \tilde{\mathbf{x}}_\epsilon^*(k)\right\}, \tag{14}$$

where the second term in (12) does not contribute to (14) since the data is assumed to be independent from the noise and the channel state. Since the information symbols are assumed to be independent, the summation in (8) contributes only the $l' = 0$ term. Thus, we have

$$\begin{aligned} E\left\{a_m \lambda_{ik'}\right\} &= \boldsymbol{\hbar}_i E\left\{a_m \mathbf{X}_0^*\right\} \mathbf{g}_\epsilon(k) \\ &= \boldsymbol{\hbar}_i \bar{\mathbf{\Gamma}}_m \mathbf{g}_\epsilon(k), \end{aligned} \tag{15}$$

where we have let $\bar{\mathbf{\Gamma}}_m = E\left\{a_m \mathbf{X}_0^*\right\}$. Similarly, defining $\bar{\mathbf{\Gamma}}'_m = E\left\{a_m \mathbf{X}_0\right\}$, results in

$$\begin{aligned} E\left\{a_m \lambda_{ik'}^*\right\} &= \boldsymbol{\hbar}_i^* E\left\{a_m \mathbf{X}_0\right\} \mathbf{g}_\epsilon(k) \\ &= \boldsymbol{\hbar}_i^* \bar{\mathbf{\Gamma}}'_m \mathbf{g}_\epsilon(k). \end{aligned} \tag{16}$$

Using (15) and (16), we take the expectation of both terms in (10), giving

$$E\left\{a_1 \tilde{s}_0\right\} = \frac{1}{\|\mathbf{H}\|^2}\left(\boldsymbol{\hbar}_1^* \bar{\mathbf{\Gamma}}'_1 \mathbf{g}_\epsilon(0) + \boldsymbol{\hbar}_2 \bar{\mathbf{\Gamma}}_1 \mathbf{g}_\epsilon(1)\right) \tag{17}$$

and

$$E\left\{a_0 \tilde{s}_1\right\} = \frac{1}{\|\mathbf{H}\|^2}\left(\boldsymbol{\hbar}_2^* \bar{\mathbf{\Gamma}}'_0 \mathbf{g}_\epsilon(0) - \boldsymbol{\hbar}_1 \bar{\mathbf{\Gamma}}_0 \mathbf{g}_\epsilon(1)\right). \tag{18}$$

Letting $\rho \triangleq E\left\{a_m^2\right\}$, it can easily be shown that

$$\bar{\mathbf{\Gamma}}_0 = \begin{bmatrix} 1 & 0 \\ 0 & \rho \end{bmatrix}, \bar{\mathbf{\Gamma}}_1 = \begin{bmatrix} 0 & -\rho \\ 1 & 0 \end{bmatrix} \tag{19}$$

and

$$\bar{\mathbf{\Gamma}}'_0 = \begin{bmatrix} \rho & 0 \\ 0 & 1 \end{bmatrix}, \bar{\mathbf{\Gamma}}'_1 = \begin{bmatrix} 0 & -1 \\ \rho & 0 \end{bmatrix}. \tag{20}$$

Substituting (19) and (20) into (17) and (18), and noting that $\mathbf{g}_\epsilon(0) = [g(\epsilon), g(\epsilon - T)]^T$ and $\mathbf{g}_\epsilon(1) = [g(\epsilon + T), g(\epsilon)]^T$, through the use of (10) one obtains

$$\begin{aligned} E\left\{\hat{\epsilon}\right\} &= \frac{1}{\|\mathbf{H}\|^2}\left\{\boldsymbol{\hbar}_2^*\begin{bmatrix} \rho g(\epsilon) \\ g(\epsilon - T) \end{bmatrix} - \boldsymbol{\hbar}_1\begin{bmatrix} g(\epsilon + T) \\ \rho g(\epsilon) \end{bmatrix}\right. \\ &- \left.\boldsymbol{\hbar}_1^*\begin{bmatrix} -g(\epsilon - T) \\ \rho g(\epsilon) \end{bmatrix} - \boldsymbol{\hbar}_2\begin{bmatrix} -\rho g(\epsilon) \\ g(\epsilon + T) \end{bmatrix}\right\}. \end{aligned} \tag{21}$$

After inserting (13), collecting all terms and simplifying, (21) reduces to

$$E\left\{\hat{\epsilon}\right\} = \frac{1}{\|\mathbf{H}\|^2}\sum_{j=1}^{n_R}\left(|h_{1j}|^2 + |h_{2j}|^2\right)\left(g(\epsilon - T) - g(\epsilon + T)\right).$$

Finally, noting that

$$\|\mathbf{H}\|^2 = \sum_{j=1}^{n_R} |h_{1j}|^2 + |h_{2j}|^2,$$

we obtain

$$\begin{aligned} E\left\{\hat{\epsilon}\right\} &= E\left\{a_0\tilde{s}_1 - a_1\tilde{s}_0\right\} \\ &= g(\epsilon - T) - g(\epsilon + T). \end{aligned} \tag{22}$$

Thus, the detector uses the difference in threshold crossings to estimate the timing offset ϵ. The expression obtained in (22) is the same as that derived in [8] for PAM signals. It is important to note that in the presence of fading, which was not considered by [8], the detector given by (10) yields a reliable estimate regardless of the state of the channel. The above result holds true in the sense of the statistical average over the data. In practice the timing loop approximates the statistical average with a time average over the data symbols. Complete channel state information is also assumed.

After initial timing acquisition is performed (typically using a known training sequence), the receiver must track the timing drift without the knowledge of the transmitted data symbols. In place of the information symbols, the TED uses the outputs of the decision device. The resulting decision-directed (DD) TED is given by

$$\hat{\epsilon}_{DD} = \hat{a}_0\tilde{s}_1 - \hat{a}_1\tilde{s}_0, \tag{23}$$

where $\hat{a}_0$ and $\hat{a}_1$ are the decision device outputs corresponding to the data symbols within a block.

IV. Timing Correction

We now outline a method for correcting the sampling epoch based on the timing error estimate produced by the TED derived in Section III.

Let the timing offset during block l be expressed as

$$\epsilon_l = \tau_l - \hat{\tau}_l,$$

where τ_l is the timing delay relative to the receiver time axis and $\hat{\tau}_l$ is the timing correction introduced by the receiver based on the TED output for block l given by (23). To minimize the effects of noise, the timing error estimate $\hat{\epsilon}_l$ is passed through a first-order IIR filter with a 3 dB bandwidth set according to the timing drift being tracked. We denote the filtered error signal by $\hat{\epsilon}'_l$. If $\hat{\epsilon}'_l$ exceeds some threshold value ϵ_{th}, the timing correction $\hat{\tau}_l$ is adjusted by a fraction of the symbol interval T/Q, depending on the polarity of the error estimate,

$$\hat{\tau}_{l+1} = \begin{cases} \hat{\tau}_l + T/Q, & \tilde{\epsilon}'_l > \epsilon_{th} \\ \hat{\tau}_l - T/Q, & \tilde{\epsilon}'_l < -\epsilon_{th} \end{cases}. \tag{24}$$

V. Simulation Results

Having derived the TED, we now evaluate its tracking performance in 1-, 2- and 4- antenna receivers. We present results in the form of SER and timing MSE, as well as determine the timing bandwidth range for which the receiver is able to maintain timing lock. The data symbols were encoded using the Alamouti code matrices given in (1), (2) and (3). The encoded symbols were then passed through an RRC pulse shaping filter with a rolloff factor of $\beta = 0.35$. The simulations were carried out using a resolution of $T/8$, that is filtering at both the transmitter and the receiver was done using waveforms sampled at that rate.

The channel was assumed to be quasi-static, frequency-flat Rayleigh fading with a normalized Doppler frequency $f_D T = 0.01$, and independent on each diversity branch. Note that the derivation of the TED in Section III assumed that channel was constant during all blocks contributing to ISI. This assumption was relaxed for the simulations, where the channel was kept constant for the duration of one code block, that is for N=2 symbol intervals. The data was then corrupted by additive white Gaussian noise (AWGN).

The received signal was match filtered on each receiver branch. The timing drift was simulated by periodically perturbing the sampling phase in a 'random walk' fashion, that is randomly advancing or delaying the sampling in increments of $T/8$ every N_τ symbol intervals. Thus, the timing error bandwidth, normalized to the symbol duration T, given by

$$B_\tau T = \frac{T/8}{N_\tau T} = \frac{1}{8N_\tau}.$$

The data was then decoded according to (9) assuming perfect channel knowledge at the receiver. As we consider the tracking performance, the data symbols were unknown to the receiver and the timing error estimation was performed using a DD TED given by (23). The timing error estimate $\hat{\epsilon}_l$ was passed through a first order IIR filter, resulting in the filtered output $\tilde{\epsilon}'_l$ given by

$$\tilde{\epsilon}'_l = \alpha\tilde{\epsilon}'_{l-1} + (1-\alpha)\tilde{\epsilon}_l$$

with $\alpha = 0.9$. The signal $\tilde{\epsilon}'_l$ was then used to control the sampling phase according to (24). The simulation results were obtained by transmitting 5×10^4 data symbols and averaging over 100 trials. The timing was assumed to be synchronized at the start of the transmission.

A. SER Performance

Figures 1 and 2 show BPSK and QPSK symbol-error rate results for normalized timing drift bandwidth $B_\tau T = 1 \times 10^{-4}$ and $B_\tau T = 5 \times 10^{-4}$. The error threshold ϵ_{th} was set to 0.4, 0.3 and 0.2 for $n_R = 1$, 2 and 4, respectively. The value of ϵ_{th} was increased for lower diversity orders in order to insure stability of the timing synchronization at low SNR. SER performance curves for ideal timing synchronization are provided as a reference.

The results demonstrate that the receiver is able to track the timing variation with a very small performance drop. For

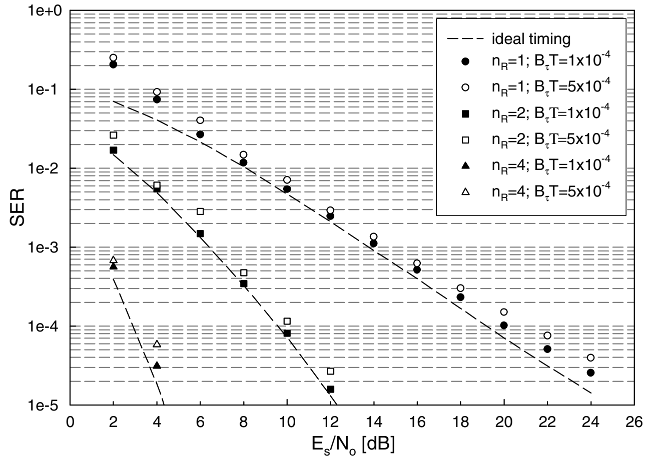

Fig. 1. BPSK SER Performance ($n_T = 2$, $f_D T = 0.01$)

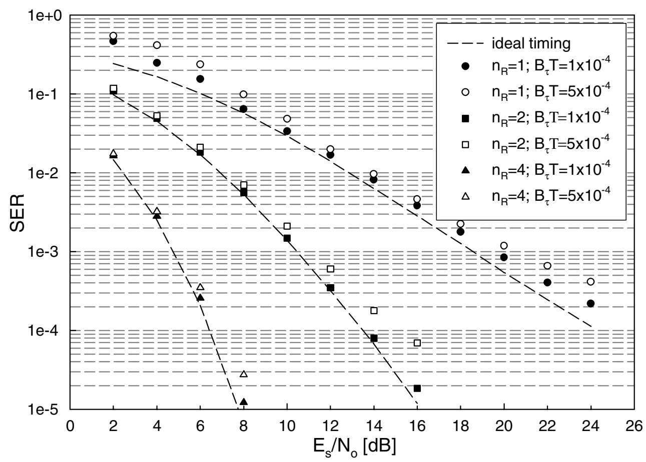

Fig. 2. QPSK SER Performance ($n_T = 2$, $f_D T = 0.01$).

$n_R = 1$, a drop of $2-4$ dB is observed in the low SNR region, where the effects of noise as well as the incorrect data decisions affect the reliability of the TED output.

At high SNR, the timing drift contributes to a slight SER floor. As will be shown in subsequent sections, this error floor can be significantly reduced by lowering the value of error threshold ϵ_{th}, or alternatively, the loop filter coefficient α. Decreasing these parameters would result in a more responsive error tracking. It is important to note, however, that decreasing either ϵ_{th} or α, results in reduced stability at low SNR, where the effects of noise on the output of the TED are more significant. A method of ensuring stability at low SNR and good high SNR performance would be to gradually lower α and ϵ_{th} with increasing SNR. This would require the receiver to estimate the signal strength.

We note that the algorithm proposed here is more stable to that considered in [7], where it was necessary to freeze the timing correction during deep fades, when the TED output was unreliable. In contrast, because the TED proposed in this paper is robust to channel fading, the timing loop can be enabled at all times.

B. Performance as a Function of Timing Bandwidth

We now determine the range of timing drift bandwidth for which the receiver is able to maintain a timing lock. Figure 3 shows SER performance as a function of $B_\tau T$ for various values of error threshold ϵ_{th}. The results were obtained for an $n_R = 2$ QPSK system operating at $SNR = 10$ dB.

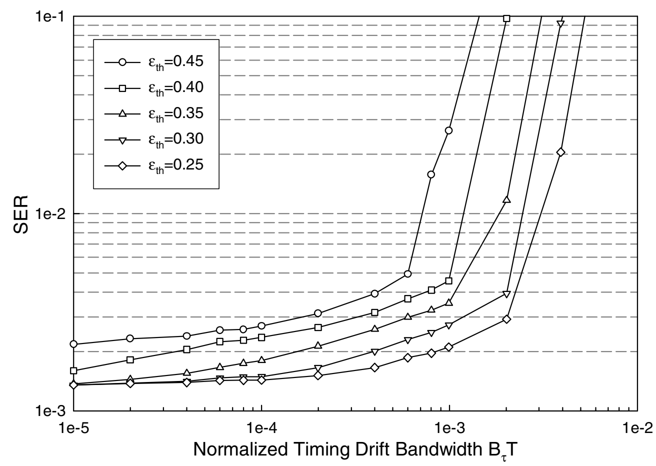

Fig. 3. SER vs $B_\tau T$ for varying ϵ_{th} (QPSK, $n_R = 2$, $E_s/N_0 = 10$ dB).

From the Figure 3 we see that the receiver is able to track the timing up to $B_\tau T$ = 0.001, which corresponds to a relatively fast timing drift where an offset of T is introduced every 1000 symbol intervals. At a reasonably high SNR, the effect of lowering the error threshold ϵ_{th} is two-fold. As mentioned in Section V-A, decreasing ϵ_{th} results in a more responsive timing loop, giving better SER performance. In addition, lowering the error threshold increases the range of timing bandwidth. While not shown here, similar effect can be achieved by lowering the value of α, that is increasing the bandwidth of the loop filter.

C. Timing Mean Square Error Performance

Finally, we examine the timing MSE performance of the proposed receiver. Figure 4 shows the MSE as a function of the timing error bandwidth $B_\tau T$ for the same parameter set as in Section V-B (QPSK, $n_R = 2$, $SNR = 10$ dB). As hinted by the results presented in Figure 3, we see that the timing MSE can be reduced by lowering the error threshold ϵ_{th}. Compared to the SER, the timing MSE is significantly more sensitive to the timing recovery parameters, where a drop of up to 2 orders of magnitude can be achieved by adjusting ϵ_{th}.

Previous methods of timing synchronization, specifically those proposed by [5] and [6], achieved an asymptotic MSE performance greatly dependent on the oversampling rate used. For oversampling rate of $Q = 4$, algorithm in [6] results in MSE on the order of 2×10^{-5}, with a further reduction for higher values of Q. The algorithm proposed here, which does not require any oversampling, achieves MSE on the order of 1×10^{-4}, or lower, depending on the values of ϵ_{th} and α used.

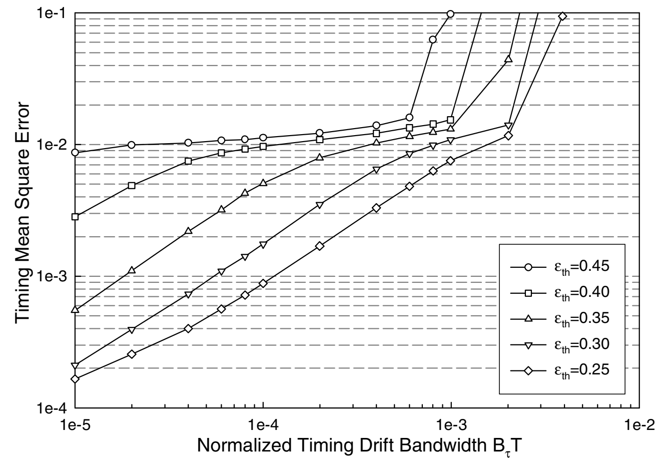

Fig. 4. MSE vs $B_\tau T$ for varying ϵ_{th} (QPSK, $n_R = 2$, $E_s/N_0 = 10$ dB).

VI. Conclusion

We have presented a very low-complexity timing error detector for $n_T = 2$ OSTBC M-PSK systems. We have shown that the TED uses the difference in threshold crossings similarly to the Mueller and Muller Detector. Apart from its simplicity, the key property of the detector is its robustness to the effects of fading. Simulation results evaluating SER performance in the presence of Rayleigh fading were presented. The receiver is able to maintain timing lock for high rates of timing drift (up to $B_\tau T$ = 0.001). Finally, MSE performance of the timing recovery algorithm was evaluated.

Acknowledgment

The authors would like to thank NSERC of Canada and the Bell Mobility / Samsung Grant on Smart Antennas at Queen's University for their support of this research.

References

[1] S.M.Alamouti. A simple transmit diversity technique for wireless communication. *IEEE J. Select. Areas Commun.*, 16(8):1451–1458, October 1998.

[2] V.Tarokh, N.Seshadri, and A.R.Calderbank. Symbol-timing synchronization in space-time coding systems using orthogonal training sequences. *IEEE Trans Inf. Theory*, 44:744–765, March 1998.

[3] V.Tarokh, H.Jafarkhani, and A.R.Calderbank. Space-time block coding for wireless communications: performance results. *IEEE J. Select. Areas Commun.*, 17:451–460, March 1999.

[4] A.F.Naguib, V.Tarokh, N.Seshadri, and R.Calderbank. A space-time coding modem for high-data-rate wireless communications. *IEEE J. Select. Areas Commun.*, 16(8):1459–1478, October 1998.

[5] Y.-C.Wu and S.C.Chan. On the symbol timing recovery in space-time coding systems. In *Proc. IEEE WCNC*, March 2003.

[6] Y.-C.Wu, S.C.Chan, and E.Serpedin. Symbol-timing synchronization in space-time coding systems using orthogonal training sequences. In *Proc. IEEE WCNC*, March 2004.

[7] P.A.Dmochowski and P.J.McLane. Joint timing and pilot symbol channel estimation for diversity receivers in rayleigh fading channels. In *Proc. IEEE PIMRC*, September 2004.

[8] K.H.Mueller and M.Muller. Timing recovery in digital synchronous data receivers. *IEEE Trans Commun.*, COMM-24:516–531, May 1976.

[9] G.Ganesan and P.Stoica. Space-time block codes: A maximum SNR approach. *IEEE Trans Inf. Theory*, 47(4):1650–1656, May 2001.

[10] G.L.Stuber. *Principles of Mobile Communications*. Kluwer Academic Publishers, Boston, 2001.